Growth and magnetic properties of stoichiometric and site-disordered single crystalline MgV_2O_4

A. T. M. Nazmul Islam,[1,*] Elisa M. Wheeler,[1] Manfred Reehuis,[1] Konrad Siemensmeyer,[1] Michael Tovar,[1] Bastian Klemke,[1] Klaus Kiefer,[1] Adrian H. Hill,[2] and Bella Lake[1,3]

[1]*Helmholtz-Zentrum Berlin für Materialien und Energie GmbH, Magnetism and Superconductivity of Quantum Materials, Hahn-Meitner-Platz 1, D-14109 Berlin, Germany*

[2]*European Synchrotron Radiation Facility, 6 rue Jules Horowitz, BP 220, 38043 Grenoble Cedex 9, France*

[3]*Institut für Festkörperphysik, Technische Universität Berlin, Hardenbergstraße 36, D-10623 Berlin, Germany*

(Received 29 August 2011; revised manuscript received 16 December 2011; published 10 January 2012)

We have grown several single crystals of the highly frustrated $S = 1$ spinel MgV_2O_4 using different starting compositions and growth conditions. From our study of their physical properties by magnetic susceptibility, heat capacity, and single-crystal neutron and powder-diffraction measurements, we observe that a minute amount of disorder suppresses the structural and magnetic phase transitions. As little as 3% disorder in the octahedral site introduced random strain, which was enough to completely suppress the transitions and induce a spin-glass phase at low temperatures. We believe that the reason is spin-exchange disorder rather than disorder in the weakly diluted magnetic lattice. Our results also show that the MgO-V_2O_3 system is a solid solution that melts slightly incongruently, and we demonstrate that by using an optimized solvent in the traveling-solvent floating-zone configuration a large single crystal ($l = 25$ mm, $d = 6$ mm) with a homogeneous composition, free of site disorders can be grown.

DOI: 10.1103/PhysRevB.85.024203 PACS number(s): 81.10.Fq, 61.43.−j, 75.50.Lk

I. INTRODUCTION

Highly frustrated magnets are ideal systems to investigate novel quantum magnetic states. A key feature of frustrated magnets is the suppression of long-range magnetic order to temperatures well below the Curie-Weiss temperature. Cubic spinels (chemical formula AB_2O_4) with a transition metal ion in the B-site form such magnets, since the B-site magnetic ions lie on a network of corner-sharing tetrahedra (Fig. 1) creating a three-dimensional magnet where nearest-neighbor magnetic interactions are potentially competing. In vanadate spinels the A site is occupied by a divalent metal, such as Cd^{2+}, Zn^{2+}, Mn^{2+}, Mg^{2+}, and is surrounded by an oxygen tetrahedron, while the octahedral B site is filled by V^{3+} ions, which have two t_{2g} electrons and a spin value $S = 1$. The V^{3+} ions realize a geometrically frustrated quantum magnetic structure with strong antiferromagnetic interactions between nearest neighbors arising via direct overlap of the t_{2g} orbitals. These systems have attracted intensive research in recent years as they are ideal systems to study the subtle interaction between spin, lattice, and orbital degrees of freedom and their role in the development of magnetic order.[1–4]

However, spinels are not always in their ideal configuration, with divalent A cations in the tetraheadral site and trivalent B cations in the octahedral site. In fact, significant octahedral-tetrahedral disorder of A and B cations is so common that such spinels are often expressed as a mixture of the ordered and inverse state described by the general formula $^{[4]}(A_{1-x}B_x)^{[6]}(B_{2-x}A_x)O_4$, where x is the occupancy of cation B (in our case V^{3+}) at the tetrahedral site. In particular, magnesium vanadates show a high degree of disorder because the binary join between the end members MgV_2O_4 and Mg_2VO_4 in the system $Mg_{2-x}V_{1+x}O_4$ exhibits complete miscibility over the entire range ($0 \leqslant x \leqslant 1$), which can also coexist with MgO. The composition has a strong dependence on the oxygen partial pressure p_{O2} of the environment used during synthesis when x approaches unity.[5]

The site disorder in MgV_2O_4 spinel can be classified into two types. The first type concerns site disorder on only the octahedral site, where the magnetic ions are partially replaced by a nonmagnetic ion. This is expected to disrupt the magnetic lattice and induce a spin-glass state in the system. Mamiya *et al.* demonstrated that a spin-glass phase is observed above 10% substitution of nonmagnetic Al^{3+} for V^{3+} in MgV_2O_4.[6,7] Octahedral site disorder in magnesium vanadate can also occur by cation mixing. The V^{3+} ions with spin $S = 1$ are replaced with the cation-associate, V^{4+}-Mg^{2+}, on the octahedral sites.[8] Partial doping by V^{4+}, which has $S = \frac{1}{2}$ and nonmagnetic Mg^{2+}, might be expected to reduce the frustration in the magnetic system by disruption of the tetrahedral network of V^{3+} ions. The second kind of disorder in which only the tetrahedral site is affected by vacancy or doping by a nonmagnetic ion may seem irrelevant to the magnetic lattice, but it can affect the local octahedral environment and hence the lattice topology and spin correlations in the system.[9] Due to these complex states, magnesium vanadates are not considered to be simple binary metal-nonmetal systems but instead as complicated ternary metal-metal-nonmetal systems. The site-disordered states are more favorable at high temperature when the system re-equilibrates by a process described as nonconvergent since there is no change of symmetry upon disordering.[10] Therefore the thermal history and atmosphere during the sample preparation process have a strong influence on the cation distribution and site disorder and are expected to have a significant effect on the physical properties of different samples. In its stoichiometric composition, free of any structural disordered state, MgV_2O_4 undergoes two phase transitions upon cooling. First a structural transition from cubic to tetragonal symmetry at $T_S \approx 65$ K and then a magnetic transition around $T_N \approx 42$ K to long-range antiferromagnetic order.[4,7] However, growth of a large single crystal of MgV_2O_4 without cation disorder and good compositional homogeneity is considered extremely challenging.[8]

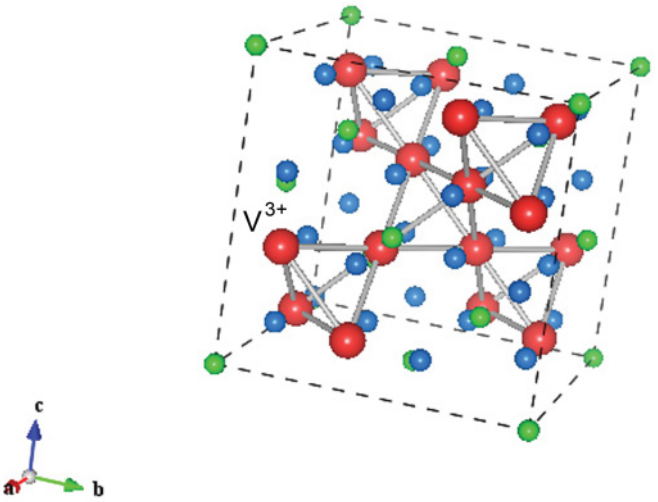

FIG. 1. (Color online) Geometrically frustrated structure of corner-sharing tetrahedra of V^{3+} ($S = 1$) in the cubic spinel MgV_2O_4 lattice.

We have grown several large single crystals of MgV_2O_4 varying the starting composition and feed-rod preparation conditions with an aim to optimize the growth conditions. Physical properties of these crystals such as magnetic susceptibility, heat capacity, and crystal stoichiometry were studied with an aim to understand the influence of cation site order-disorder. Finally, we report growth of a large single crystal ($l = 25$ mm, $d = 6$ mm) with a homogeneous composition, free of site disorders, and which shows two sharp transitions at the expected temperatures.

II. EXPERIMENTAL DETAILS

A. Powder preparations and crystal growths

High purity powders of V_2O_3 (Puratronic 99.97%, MV Labs) and MgO (Puratronic 99.995%, Alfa Aesar) were mixed thoroughly with an initial 1:1 molar ratio for the crystal growth. After mixing, the powder was calcinated in an alumina crucible in flowing Ar-H_2 (4%) mixture at 1000 °C for 12 hours in a vacuum furnace. The powder was then packed in a rubber tube making the total length of ∼7–8 cm and ∼6 mm in diameter. The tube with powder was then pressed hydrostatically up to 3000 bars in a cold isostatic pressure (CIP) machine. The feed rod was then sintered at 1100 °C for 24 hours in flowing Ar-H_2 (4%) mixed atmosphere. We observed that the starting composition of the powder and the conditions during the powder and feed-rod sintering have a pronounced effect on the characteristics on the growth and the properties of as-grown crystals. For this reason we prepared several batches of powder with slightly varied composition in order to find the optimum growth condition. Growths were carried out in an optical image furnace (CSI FZ-T-10000-H-VI-VP, Crystal Systems, Inc., Japan) equipped with four 1000 W tungsten halide lamps focused by four ellipsoidal mirrors. The feed rod was suspended from the upper shaft using platinum wire, while another small feed rod was fixed to the lower shaft to support the melt. Crystal growths were performed in flowing argon at a typical growth rate of about 10–20 mm/h. Our different growths are described in order as follows:

Growth-1: A composition with 1% excess V_2O_3 was added in the starting material based on previous reports of growths of CaV_2O_4[11] and MnV_2O_4,[12] where excess V_2O_3 was used to compensate for evaporation during growth. During this first growth, we also observed that the evaporation of V_2O_3 is dependent on the quality of the argon atmosphere used. Additionally, there was a considerable amount of Mg evaporation during the growth. We believe this was due to decomposition of some MgO in the presence of H_2 in the atmosphere during the powder and feed-rod preparation processes where an atmosphere of Ar-H_2 (4%) was used.

Growth-2: To compensate for the decomposition of some MgO during the powder and feed-rod preparation, a composition with 3% excess MgO was used.

Growth-3: An adjustment of the excess MgO to 1% was used to compensate for the MgO decomposition and a very low flow rate of Ar-H_2 (4%) gas was maintained to reduce the exposure of powder and feed rod to fresh H_2 gas. Additionally, an argon gas purifier (NuPure Eliminator) was installed in the gas inlet line of the floating-zone (FZ) machine to ensure the maximum purity of the Ar flow into the growth chamber. An oxygen gas detector installed in the gas outlet of the FZ machine confirmed that the oxygen content in the atmosphere of the growth chamber was below 1 ppb at high temperatures.

Growth-4: A traveling-solvent floating-zone (TSFZ) growth was carried out, which utilized the zone-leveling technique in order to obtain a large single crystal with a homogeneous composition. A feed rod with the same composition as that of Growth-3 and a solvent of composition with 3% excess V_2O_3 was used for this growth.

In all cases a seed crystal from a previous growth was used for subsequent crystal growths to avoid random nucleation and obtain one large single crystal.

B. Characterization

Single crystals of MgV_2O_4 were first checked with polarized optical microscopy, scanning electron microscopy, energy dispersive x-ray spectroscopy, and x-ray Laue diffraction to confirm that they were free of grain boundaries and pure in phase.

Neutron powder-diffraction measurements were done using the E9 high-resolution powder diffractometer at the BER II reactor at the Helmholtz-Zentrum Berlin (HZB) with an incident neutron wavelength $\lambda = 1.79$ Å (Ge). The powder samples (obtained by grinding the single crystals) were mounted on a flat sample holder, oscillating continuously in the horizontal plane to minimize preferred orientation effects, and measured for 16 hours each. The powder patterns were fitted by the Rietveld method to determine the phase purity and the crystal structure. Single-crystal neutron-diffraction experiments were carried out on three high-quality single crystals with volumes of 55 mm^3 (Growth-1), 279 mm^3 (Growth-2), and 140 mm^3 (Growth-3). The measurements were done on the four-circle diffractometer E5, at the HZB, where neutron wavelengths $\lambda = 0.89$ Å (Cu) and $\lambda = 2.36$ Å (pyrolytic graphite) were used. Powder and single-crystal neutron-diffraction data was used to determine accurately the

structural parameters and the site disorder in the system, with the help of the FULLPROF and Xtal programs.[13,14] Powder x-ray diffraction measurements were made using the high resolution diffractometer ID31 at the European Synchrotron Radiation Facility with $\lambda = 0.4$ Å at 300 K and with a Cu-$K_{\alpha 1}$ source Huber Guinier G670 diffractometer $\lambda = 1.5406$ Å. In addition temperature-dependent susceptibility and temperature-dependent heat capacity were measured in a SQUID magnetometer (Quantum Design MPMS) and in a Physical Property Measurement System (PPMS, Quantum Design), respectively, in the Laboratory of Magnetic Measurements (LaMMB) in HZB.

III. RESULTS

A. Crystal growth

As-grown single crystals from different growths are shown in Fig. 2. All the crystals have a shiny surface with a metallic luster. In Growth-1 [Fig. 2(a)] there was a considerable amount of volatilization of metallic Mg at lower temperatures (around 1100 °C) and evaporation of some vanadium oxide at higher temperatures. We believe that during the powder and feed-rod preparation process some amount of MgO decomposed because of molecular H_2 in the atmosphere. The evaporation of vanadium oxide is probably due to the presence of some small amount of oxygen in the growth atmosphere of Ar (purity of 5N). Even a minute presence of O_2 in the atmosphere can lead to oxidation of some vanadium oxides, which, because they have a lower melting temperature, can evaporate more easily at the higher melting temperatures of MgV_2O_4.

In Growth-2 [Fig. 2(b)] we used 3% excess MgO in the starting powder to compensate for the decomposed MgO during powder preparation. Our single-crystal neutron-diffraction experiments, shown later, demonstrate that this amount of MgO overcompensated and there was an excess amount of MgO in the single crystal. We concluded that although an Ar-H_2 atmosphere is essential to stabilize the V_2O_3 powder in its 3+ oxidation state, the gas flow rate needs to be optimized to limit the exposure of MgO to molecular H_2 so that the excess MgO in the starting material can be reduced.

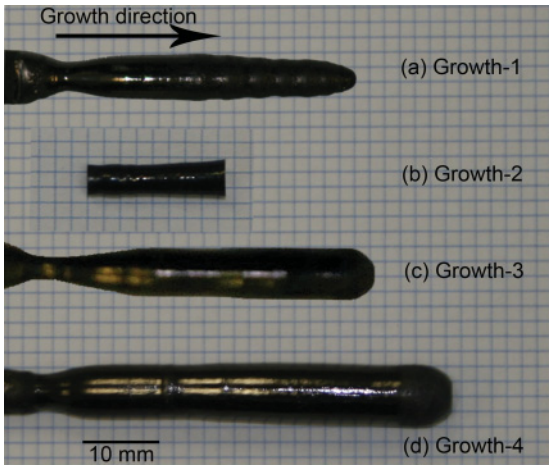

FIG. 2. (Color online) As-grown single crystals grown in the FZ machine from different starting compositions.

In Growth-3 [Fig. 2(c)] we observed significantly reduced evaporation of materials from the melt, which is a result of both optimization of the gas-flow rate during powder and feed-rod sintering and the use of O_2 eliminator in the Ar gas line of the FZ machine. Prevention of decomposition and evaporation of materials in different steps of the crystal-growth process was essential to have better control over the actual composition of the crystal, which itself is a solid solution. A seed crystal oriented along one of the cubic crystallographic axis was used in this growth. We found that the whole as-grown crystal grew epitaxially with a length of 45 mm and a diameter of ∼6 mm, as confirmed by x-ray Laue diffraction patterns taken at several points along the crystal. Our bulk properties' measurements showed that the composition of crystal actually changed continuously along the growth direction during the crystal growth, as is expected in a solid solution that solidifies at a slightly different composition from melt composition.

Figure 2(d) shows the single crystal grown by the TSFZ method (Growth-4). A stable-growth stage was achieved with low evaporation of materials during the growth. The as-grown single crystal was found to have grown epitaxially along the crystallographic a-axis with a diameter of ≈5–6 mm and length of 45 mm.

B. Susceptibility and heat capacity

Susceptibility and heat capacity measurements of Growth-1, -2, and -3 are shown in Fig. 3. Growth-1 shows multiple features at 55 K, 49 K, and 37 K in the temperature-dependent magnetic-susceptibility measurement. The temperature-dependent heat-capacity measurement on the same sample shows a spike at 55 K, a shoulder around 49 K, and a weak broad peak at 37 K. Conversely, Growth-2 does not show any anomalies in the heat-capacity measurements, and the susceptibility measurement has a single transition at a temperature $T_F \approx 12.5$ K. About this temperature, the field-cooled and zero field-cooled susceptibility appear to diverge, suggesting that for $T < T_F$ there is spin freezing. We propose the susceptibility shows spin-glass behavior at lower temperatures, although no broad features about T_F are discernable in the heat capacity. Susceptibility measurements on different cuts of the Growth-3 crystal show changes in structural and magnetic transitions along the growth direction. The lower part shows $T_S \approx 55$ K, $T_N \approx 38$ K, and the upper part shows $T_S \approx 65$ K, $T_N \approx 42$ K. In between these two parts a region having both sets of transitions can be observed. This is due to a change of composition throughout the length of the growth. Change of composition also proves that the MgO-V_2O_3 is a binary solid solution that melts incongruently, where the composition is changed while crystallizing from the melts. We have chosen a 6-mm part of the length of the crystal having a uniform composition defined by only two sharp transitions at 65 K and at 42 K as observed in both the susceptibility and heat capacity measurements from thin slices of crystal from either side of this piece. The two sharp transitions are due to the structural transition (at $T_S = 65$ K) and magnetic ordering (at $T_N = 42$ K) to an antiferromagnetic state, as shown in our previous work.[4] The end part of the crystal has a rough surface, which is due to excess V_2O_3 inclusions in the crystal.

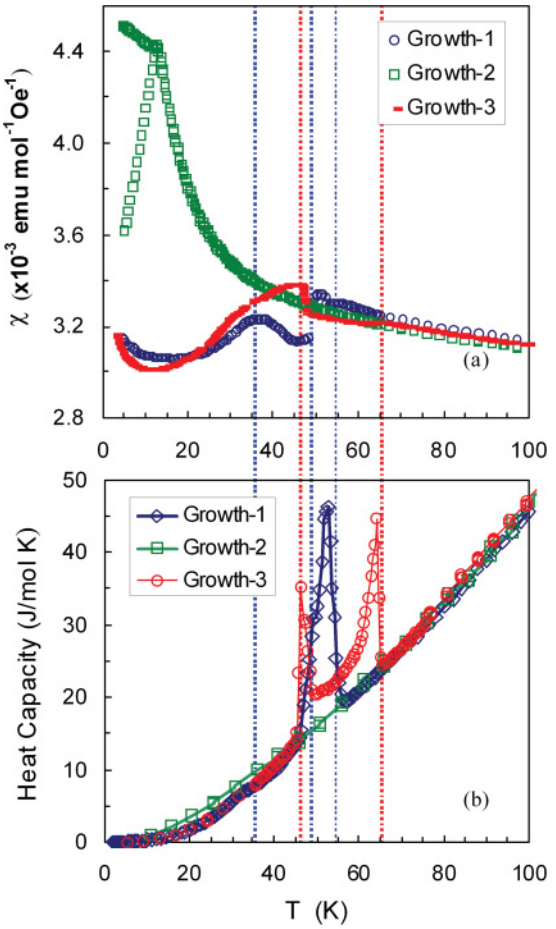

FIG. 3. (Color online) Temperature dependence of susceptibility (a) and heat capacity (b) of different MgV_2O_4 crystals. The vertical dotted lines are guides for the structural and magnetic transitions observed in Growth-1 and Growth-3 by single-crystal neutron-diffraction measurements.

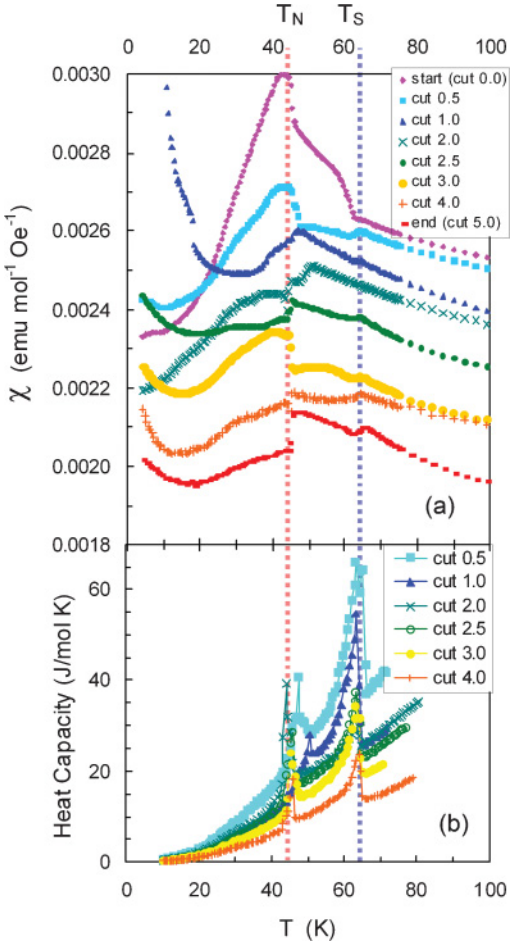

FIG. 4. (Color online) Temperature dependence of magnetic susceptibilites (a) and heat capacity (b) of different pieces of Growth-4 along the growth direction. (Plots are shifted slightly in the y-axis for clarity). The vertical dotted lines indicate the structural transition T_S and magnetic transition T_N observed in a homogeneous crystal free of disorder.

Growth-4 also shows variation along part of its length, see Fig. 4. Heat capacity measurements made on different sections of the crystal show variation in the transition temperatures. Cuts of small pieces of crystals were taken at approximately even distances along the full length of Growth-4. The region from the start until cut 2.0 shows some variation in transition temperatures. We believe that this is due to the compositional fluctuations in the initial state of the growth that lasts until an equilibrium state is reached. We observe that the susceptibilities and heat capacity in the region between cut 2.5 and cut 5.0 (end) show identical characteristics in the transitions. There is a single set of structural and magnetic transitions for all cut-crystals in this region coinciding at the values of $T_S = 65$ K and $T_N = 42$ K. As a result, we believe that this part of the single crystal is stoichiometric and homogeneous in composition having no site disorder in the system.

C. Neutron-diffraction measurements

To investigate the variation in transitions in Growth-1, powder neutron-diffraction measurements were performed upon a sample of ground single crystal. The sample was cooled from room temperature to 2 K as a series of diffraction patterns were taken. The signature of the cubic- to tetragonal-phase transition is a systematic splitting of particular cubic Bragg reflections in the powder-diffraction pattern. Further it could be seen from single-crystal neutron diffraction that the intensity of strong Bragg reflections, as shown in Fig. 5 for the reflection (400), undergoes a spontaneous change of intensity at the structural phase transition due to a strong change of secondary extinction in the crystal. The sample was found to be in a single tetragonal phase at 42 K and single cubic phase at 70 K. However, over a range in between these temperatures the powder appeared to be in a mixed structural phase where both sets of reflections coexisted (as shown by x-ray diffraction data, Fig. 5 inset).

For a detailed investigation of Growths 1–3, we carried out single-crystal neutron diffraction. The occupancies were determined by refining the data in the spinel space group. The results are summarized in Table I. Due to the strongly different neutron scattering lengths of vanadium ($b = -0.3824$ fm) and magnesium ($b = 5.375$ fm), we were able to determine the Mg-content at the V-site with very good accuracy. Our analysis of all the different growths shows a variation of the site disorder

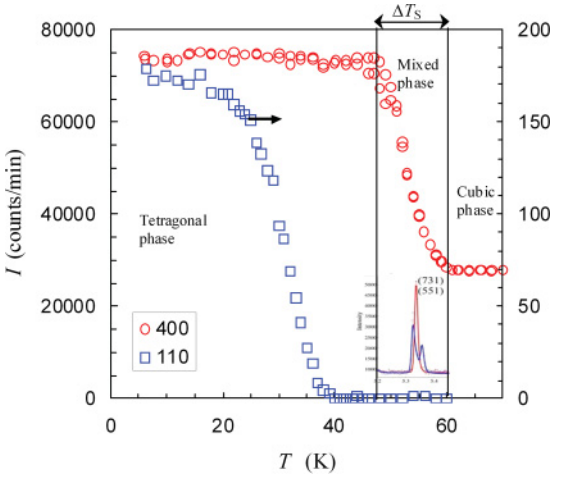

FIG. 5. (Color online) Single-crystal neutron-diffraction results for Growth-1 showing the structural (400) and magnetic (110) reflection intensities. The broad temperature range ΔT_S over which the crystal changes from cubic to tetragonal (T_S) indicates a presence of both phases simultaneously as confirmed by x-ray powder diffraction (inset). The appearance of the (110) reflection indicates the onset of magnetic ordering at $T_N = 37$ K.

between different crystals. We found that in Growth-1 both the tetrahedral site and octahedral site are only populated with Mg and V ions, respectively, and no site mixing was found. However, assuming full occupation of the Mg site, the best fit to the data indicated a slight oxygen deficiency of approximately 1.5%. For a charge-neutral compound this would imply that 4% of the octahedral sites are populated with V^{2+}. This is unlikely since the lower oxygen partial pressure required to reach this oxidation state was not used during the synthesis. A more likely explanation is a 1.3% vanadium vacancy or the presence of an undetected percentage of Mg^{2+} within the vanadium lattice. This is possible because of the uncertainty due to the small vanadium neutron scattering length. When cooling the crystal there was a large increase in intensity of the strong reflections, such as (004), as the crystal started to go through the structural phase transition at ≈60 K, which is completed at ≈48 K, as shown in Fig. 5. The structural transition over a broad temperature range indicates the range where both cubic and tetragonal phases coexist, confirming the results from powder-diffraction measurements. Below 38 K, we observed a smooth increase in intensity of new reflections with an ordering wave vector of $k = (001)$, which is associated with the onset of long-range magnetic order.

Initially for Growth-2, we also assumed that the tetrahedral site was fully populated with Mg, and that the octahedral site was solely populated with V. We found that the best fit to the data indicated only 50% of the octahedral sites were populated. This is unlikely to be the case, and we went on to assume that some Mg was also present on the octahedral sites. Due to the large contrast between the neutron-scattering power of Mg and V (V has a very small negative scattering length while that of Mg is an order of magnitude larger and positive), the measurement is very sensitive to their relative populations. The best fit gave the much more physical result that the octahedral site was partially populated with 2.9(6)% Mg and V occupying the remaining 97.1(6)%. No oxygen deficiency could be observed on the oxygen positions. It should be pointed out that this Mg would remain in its stable 2+ valence state, while the nominal valence of the Vanadium that it is replacing is 3+; therefore, to maintain charge neutrality, Mg^{2+} substitution would force an equal amount of V to change valence and become V^{4+}. Upon cooling to 5 K we observed no change in the Bragg reflections, which indicated that no transitions either structural or magnetic occurred.

For Growth-3, the single-crystal neutron-diffraction measurement was made with a piece of single crystal 6 mm in length and ≈6 mm in diameter. Our refinement shows no structural disorder in the crystal, as both tetrahedral and octahedral sites are fully populated with Mg and V ions, respectively, without any site mixing. The excess oxygen that results in the best fit of the neutron data is not significant within error. X-ray powder diffraction carried out on a ground piece of crystal shows that there is no observable discrepancy in the oxygen sites. A clear transition was observed at 64 K where the crystal structure becomes tetragonal, and long-range magnetic order was seen below 42 K, indicated by the emergence of new reflections as for Growth-1.

IV. DISCUSSION

Our measurements have shown that fine tuning of excess MgO and the composition of the growth atmosphere resulted in successful crystal growth of Magnesium Vanadate, with small impurities in the vanadium lattice causing large changes in the phase transitions of the system. This is further demonstrated by the results from the crystal grown by the TSFZ method.

From the crystal growths we observed that when the starting composition is close to stoichiometry, the composition in the crystal changes along the growth direction, as reflected in the shift in structural transition from $T_S = 55$ K in the initial part of the crystal through a region where $T_s = 55$ K and 65 K are both

TABLE I. Occupation of the *A* tetrahedral site (0.125, 0.125, 0.125), B octahedral site (0.625, 0.625, 0.625), and O site (0.26, 0.26, 0.26). For the refinement of the crystal of Growth-2 we have set the constraint $occ(V) + occ(Mg) = 1$.

	Neutron diffraction			X-ray diffraction
	Growth-1	Growth-2	Growth-3	Growth-3
A site	100% Mg	100% Mg	100% Mg	100% Mg
B site	100% V	97.1(6)%V 2.9(6)% Mg	100% V	100.6(2)% V
O Site	98.5(11)% O	99.9(10)% O	101.6(17)% O	100.2(2)% O

present to a region where $T_S = 65$ K (Growth-3). Beyond this region, although $T_S = 65$ K, the quality of the crystal degrades due to the presence of excess V_2O_3 as inclusions. This behavior in the growth points to the fact that V_2O_3 has a distribution coefficient of $\kappa < 1$, which implies that the MgO-V_2O_3 binary system is a solid solution that melts incongruently, and while cooling through the solidus line it crystallizes at a composition slightly deficient in V_2O_3 than the nominal composition. So, in order to crystallize a composition of 50 mol% V_2O_3 in MgO, a composition with excess V_2O_3 is required. Using this information we demonstrated (in Growth-4) that by using a TSFZ configuration with a V_2O_3 excess solvent on the tip of a nearly stoichiometric feed rod a *large* single crystal of MgV_2O_4 with uniform and stoichiometric composition can be grown.

The sensitivity of the crystal to defects can be seen from the earlier growths. We found that in Growth-1 an indefinable amount of site disorder suppressed the structural and magnetic transitions by about 10 K. The broad bump in the susceptibility around 38 K and 12 K below the sharp transitions may indicate microscopic inhomogeneity in this crystal. However, in Growth-2, the octahedral site disorder is large enough to suppress any transitions, both structural and magnetic, creating a spin-glass at low temperatures. Previously, a spin-glass phase has been observed in other spinel vanadates by both tetrahedral and octahedral site disorder induced by doping. Octahedral disorder created by Al doping in MgV_2O_4 shows that about 10% of isovalent Al^{3+} is required to completely suppress the transitions.[6] In the case of tetrahedral site disorder it was shown that for the $Cd_{1-x}Zn_xV_2O_4$ system it takes less than 3% of Zn to induce the spin-glass phase.[9] A spin-glass phase was also observed in Cr-spinels, where site disorder at the tetrahedral site was thought to cause stress in the lattice which led to random variations in the exchange interactions.[15] In our sample we propose that the presence of non-isovalent Mg^{2+} and V^{4+} in the octahedral site creates random variations in the exchange interactions by disrupting the vanadium environment and orbital overlap between vanadium ions. Although the classical Heisenberg nearest-neighbor antiferromagnet on a pyrochlore lattice should not show spin freezing, theoretical work on frustrated spinel lattices has shown that random variations in exchange constants can bring about spin-glass behavior. Indeed, our susceptibility measurements demonstrate that a small amount of octahedral site disorder ($\sim$3%) brings about a spin-glass transition at a temperature $T_F \approx 12.5$ K. Assuming little disorder, T_F indicates that the fluctuations in the nearest-neighbor spin exchange ($J \approx 20$ meV) are approximately 1 meV.[16] We propose that it is the spin-exchange disorder due to site disorder with a non-isovalent cation rather than the site disorder itself that reduces the transition temperature and eventually leads to suppression of structural and magnetic transitions in the system.

From the theoretical predictions of Villain *et al.*[17] the dilution of the magnetic lattice by 3% is unlikely to be the cause of the spin-glass behavior; indeed, it has been found that only with Al^{3+} above 10% substitution was a spin-glass state present at a low temperature.[6,7] In the related chromate spinels it was also shown that dilution of the magnetic lattice by Ga^{3+} resulted in smaller changes in the transition temperature than an equivalent of excess Mg^{2+} in $MgCr_2O_4$. In fact, Néel order seems to be more stable to disorder in chromates. With 4% of Mg on the Cr lattice, Néel order is still maintained at low temperatures, and no difference is observed between the zero field-cooled and field-cooled magnetic susceptibility.[18] This may well be connected to the lack of orbital degeneracy in Cr systems, which would introduce further fluctuations into the spin exchange.

This work also sheds light on inconsistences in results between powder and small single-crystal samples of ZnV_2O_4 where the powder shows clear transitions but the single crystal shows spin-glass behavior, which could simply be explained by small differences in the site disorder between these samples.[19,20] Previous studies by Mamiya and M. Onoda showed through transport measurements that 5% substitution of Al^{3+} for V^{3+} in MgV_2O_4 could suppress the transitions of MgV_2O_4.[6] Our detailed study has shown that nonmagnetic, non-isovalent Mg^{2+} has an even more pronounced effect, and by substituting V^{3+} at the octahedral site with sufficient Mg^{2+} and V^{4+} a suppression of the crystal and magnetic transitions occurs resulting in spin-glass behavior at low temperatures. We propose that this is because site-disorder, particularly by an ion of different valence, distorts the lattice and leads to a random variation in the spin exchange. We expect that the structural transition, which partially relieves frustration in the magnetically ordered phase to be very sensitive to disorder in the frustrated spin exchange couplings and might be suppressed if the frustration is relieved. The mechanism behind the structural phase transition and possible orbital ordering in MgV_2O_4 is of current interest, and this adds further evidence that the frustrated nature of the pyrochlore lattice is of importance to it.

V. CONCLUSION

In summary this work highlights that as-grown single crystals of MgV_2O_4 suffer from site-disorder, which is strongly correlated to the starting powder composition and growth conditions. The site-disorder even by a tiny amount can strongly suppress the structural and magnetic transitions, and it only takes about 3% of octahedral site disorder to induce random variation in the spin exchanges leading to a spin-glass transition in the system. Finally, it was demonstrated that by using the TSFZ technique a site-disorder free large single crystal can be grown.

ACKNOWLEDGMENTS

The authors thank D. N. Argyriou for use of the crystal growth labs.

*nazmul.islam@hmi.de

[1] O. Tchernyshyov, Phys. Rev. Letts. **93**, 157206 (2004).
[2] T. Suzuki, M. Katsumura, K. Taniguchi, T. Arima, and T. Katsufuji, Phys. Rev. Letts. **98**, 127203 (2007).
[3] T. Maitra and Roser Valenti, Phys. Rev. Letts. **99**, 126401 (2007).
[4] E. M. Wheeler, B. Lake, A. T. M. Nazmul Islam, M. Reehuis, P. Steffens, T. Guidi, and A. H. Hill, Phys. Rev. B **82**, 140406(R) (2010).

[5]H. Oshima, J. Am. Ceramic Soc. **63**, 504 (1980).
[6]H. Mamiya and M. Onoda, Solid State Commun. **95**, 217 (1995).
[7]H. Mamiya, M. Onoda, T. Furubayashi, J. Tang, and I. Nakatani, J. Appl. Phys. **81**, 5289 (1997).
[8]H. Oshima, J. Am. Ceramic. Soc. **66**, 482 (1983).
[9]Z. Zhang, D. Louca, A. Visinoiu, S.-H. Lee, J. D. Thompson, T. Proffen, A. Llobet, Y. Qiu, S. Park, and Y. Ueda, Phys. Rev. B **74**, 014108 (2006).
[10]N. Kijima, M. Toba, and Y. Yoshimura, Catal. Lett., **127**, 63 (2009).
[11]A. Niazi, S. L. Bud'ko, D. L. Schlagel, J. Q. Yan, T. A. Lograsso, A. Kreyssig, S. Das, S. Nandi, A. I. Goldman, A. Honecker, R. W. McCallum, M. Reehuis, O. Pieper, B. Lake, and D. C. Johnston, Phys. Rev. B **79**, 104432 (2009).
[12]H. D. Zhou, J. Lu, and C. R. Wiebe, Phys. Rev. B **76**, 174403 (2007).
[13]J. Rodriguez-Carvajal, Physica B **192**, 55 (1993).
[14]S. R. Hall, G. S. D. King, J. M. Stewart, Eds., *Xtal3.4 User's Manual*, University of Australia, Lamb, Perth (1995).
[15]W. Ratcliff, S. H. Lee, C. Broholm, S. W. Cheong, and Q. Huang, Phys. Rev. B **65**, 220406(R) (2002).
[16]A. Andreanov, J. T. Chalker, T. E. Saunders, and D. Sherrington, Phys. Rev. B **81**, 014406 (2010).
[17]J. Villain, Z. Phys. B **33**, 31 (1979).
[18]S. E. Dutton, Q. Huang, O. Tchernyshyov, C. L. Broholm, and R. J. Cava, Phys. Rev. B **83**, 064407 (2011).
[19]S. G. Ebbinghaus, J. Hanss, M. Klemm, and S. Horn, J. Alloys Compd. **370**, 75 (2004).
[20]M. Reehuis, A. Krimmel, N. Buttgen, A. Loidl, and A. Prokofiev, Eur. Phys. J. B **35**, 311 (2003).